

Accounts

Bio-Inspired Membranes for Advanced Polymer Electrolyte Fuel Cells. Anhydrous Proton-Conducting Membrane via Molecular Self-Assembly

Itaru Honma*[1] and Masanori Yamada[2]

[1]Energy Technology Research Institute, National Institute of Advanced Industrial Science and Technology (AIST), Tsukuba 305-8568

[2]Department of Chemistry, Faculty of Science, Okayama University of Science, Ridaicho, Okayama 700-0005

Received October 10, 2006; E-mail: i.homma@aist.go.jp

Bio-inspired materials or natural biopolymers have attracted much attention for industrial applications as biocompatible materials. Although these materials have been discarded as industrial waste around the world, there is an increasing interest in environmental, engineering, and electrical applications of the biomaterials because of their well-controlled structures and superior conducting properties. The controlled structures of the hydrogen-bonding network in biomolecules, such as bioenergetic proteins, are essential for efficient energy transduction in living systems and application of a biomolecular mechanism could make it possible to prepare efficient electrolytes with superior conducting properties. We report here a recent investigation on the new class and new concept of electrolyte materials with bio-inspired molecular architectures of acid–base pairs for anhydrous proton conduction and its application in intermediate temperature (100–200 °C) polymer electrolyte fuel cells (PEFC). Although some membranes were composed from entirely biomolecular materials, they showed large anhydrous proton conductivities from room temperature to 160 °C, and fuel cells employing biomembranes as a polymer electrolyte produced electrical power under non-humidified H_2/O_2 condition at 160 °C. These bio-inspired materials may have many potential applications not only because of its superior ion conducting properties, in particular, under anhydrous (water-free) or extremely low-humidity conditions, but also because of its biocompatibility.

Increasing interest toward the global sustainable energy has occurred in relation to political, economical, and environmental protection aspects, whereas, from an industrial development point of view, advanced energy technology is becoming intensively important recently in ordered to reduce fossil fuel consumption and keep the environment clean for human activities. The Kyoto protocol has stimulated research activities in renewable energy technology in every nation and every industrial sector. Among them, polymer electrolyte fuel cells (PEFC) have been recognized as most promising energy conversion devices because they are much very efficient and emit less of CO_2 from automobile, terrestrial, and industrial power sources.[1–3] Penetration of PEFC to the market might cause a large scale transformation of the industrial energy system, causing more efficient fossil fuel use and reduced atmospheric pollution. Also, compact and reliable PEFC units will definitely accelerate the development of eco-vehicles, typically so-called hybrid cars, in the world transportation market.[1–3] However, the current PEFC materials and system have many obstacles before they gain wide scale use: They use precious platinum electrodes and expensive Nafion® membranes, there are stability issues with Membrane-Electrode Assemblies (MEA), and managing the humidity is complicated.

The performance of the PEFC strongly depends on the nature of the electrolyte membrane.[1–14] In order to operate PEFC more effectively, membranes that are tolerant to high temperature are required, because the use of higher temperatures has various electrochemical as well as system advantages, such as the highly efficient power generation, reduced CO poisoning on the platinum surface, simplified reforming/cooling units, and co-generation. So, encouraged by these merits, many attempts have been made to develop advanced electrolyte membranes durable in an intermediate temperature range (100–200 °C), such as nano-particle impregnated Nafion®,[15–17] organic/inorganic hybrids,[18–22] engineering polyaromatic polymers,[23–28] heteropolyacids in organic silicates,[29,30] and nano-structured proton conductors.[31,32] If a membrane shows large proton conductivities in intermediate temperature range under either non-humidified or extremely low-humidified conditions, efficient PEFC operation becomes feasible. In recent years, a lot of effort has been devoted to finding new electrolyte membranes that are tolerant to high temperatures and that are conductive under dry (non-humidified) conditions, although fast proton conduction in the low-temperature regime usually necessitates the presence of mobile water molecules in the electrolytes; hydrated protons of H_3O^+ are mobile through an ion-exchanged

Published on the web November 13, 2007; doi:10.1246/bcsj.80.2110

membrane, such as Nafion®, with a liquid-like mobility.[33–35] This is why the electrolyte membrane loses its conductivities under anhydrous conditions because of the evaporation of liquid vehicle molecules. A new conducting mechanism that does not require the presence of water, but retains sufficient mobility, has been a long term challenge to overcome in the fuel cell technologies.

Here, we report our efforts to develop a new proton-conducting membrane, which has superior conducting properties than the present materials (such as Nafion® as an ion-exchanged membrane) under anhydrous conditions. In particular, an anhydrous proton-conducting membrane was synthesized by using the bio-inspired molecular systems. Self-organized molecular systems have a proton assembly arranged along its acid–base pairs and direct hopping of ions is possible along these assembled pathways. Whereas fast translocation of protons in aqueous solutions is assumed to be responsible for superior electrolytic conduction in PEFCs, the self-assembled electrochemical acid–base network provides novel conducting channels via a "hop-and-turn" or the Grotthuss mechanism, which involves chemical exchange of proton and reorganization among hydrogen-bonded molecular networks for sufficient anhydrous conductivities.[33–35]

Bio-inspired materials or natural biopolymers have attracted much attention for a industrial applications as a biocompatible material.[36–46] Although these materials are often discarded as industrial waste around the world, there is an increasing interest towards the application of the biomaterials in devices because they have well-controlled structures and superior conducting properties. The controlled hydrogen-bonded network in biomolecules, such as bioenergetic proteins, is essential for efficient energy transduction in living systems,[47,48] and these biomolecules may be efficient electrolytes with superior conducting properties. We report here a recent investigation on a new class of electrolyte materials with bio-inspired molecular architectures of acid–base pairs for anhydrous proton conduction and its application in an intermediate temperature PEFC. Although some membranes were composed from entirely biomolecular materials, they showed a large anhydrous proton conductivity from room temperature to 160 °C, and a fuel cell employing the biomembrane as a polymer electrolyte generated an electrical power under non-humidified H_2/O_2 condition at 160 °C.

1. Acid–Base Composite Materials

Recently, acid–base composite polymer materials have been considered to be polymer electrolytes of single proton conductors under intermediate temperature (100–200 °C) and anhydrous (low-humidity) conditions.[4–14] In this case, anhydrous proton transport might be based on a non-vehicular mechanism (Grotthuss mechanism), in which only protons are mobile from site to site without the assistance of diffusible water molecules.[33–35] Proton mobility in the electrolyte most likely depends on the distance between the hopping sites in the polymer material,[33–35] and usually, it is related to the activation energy of proton transfer under anhydrous condition. Several new polymers have been reported as possible electrolytes: polybenzimidazole(PBI)–acidic molecules,[49–51] imidazole group immobilized polymer–acidic molecules,[52–56] ionic liquid,[57–60]

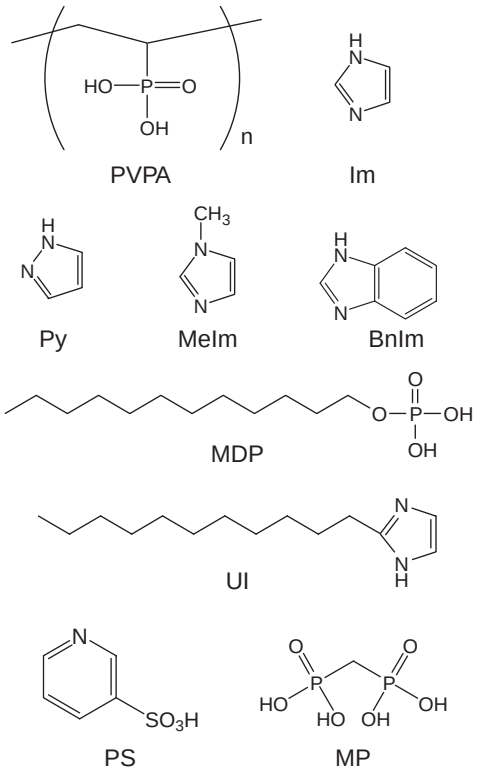

Scheme 1. Molecular structures of acid–base composite materials.

and inorganic–organic copolymers.[61] These electrolyte materials have high proton conductivity even under anhydrous and intermediate temperature conditions; however, some require the presence of liquid moieties, such as phosphoric or sulfuric acid solutions or an ionic liquid, to make proton conductivity high enough for the practical applications.

So, we prepared anhydrous proton-conducting electrolytes by employing a strong phosphonic acid polymer, poly(vinylphosphonic acid) (PVPA) or mono-dodecylphosphate (MDP), and an organic base heterocycle, such as imidazole (Im), pyrazole (Py), 1-methylimidazole (MeIm), and benzimidazole (BnIm).[62,63] These acidic and basic molecular structures are shown in Scheme 1. By tuning the combination of these acid–base pairs, it might be possible to maximize the conductivities.

Figures 1a and 1b show the thermogravimetric (TG) and differential thermal analyses (DTA, scanning rate of 10 °C min^{-1}) of (1) PVPA material, (2) PVPA–89 mol % Im, and (3) Im materials, respectively. PVPA material showed a TG weight loss, which is due to the evaporation of water from the membrane, of ca. 5% at 150 °C. In contrast, we have reported in our previous paper[63] that the TG weight loss of a PVPA–Im composite material decreases with an increase in the Im mixing ratio and that, the endothermic peak due to the evaporation of water also decreases with an increasing in the mixing ratio of Im molecules. Interestingly, for the composite electrolyte materials, the melting of Im molecule itself was not observed when interacting with acidic phosphonic groups in the solid polymer materials, resulting in stable solids above the melting points. The enhanced structural stability of PVPA–Im composite materials, even at intermediate temperatures (<160 °C), implies the existence of strong acid–base interac-

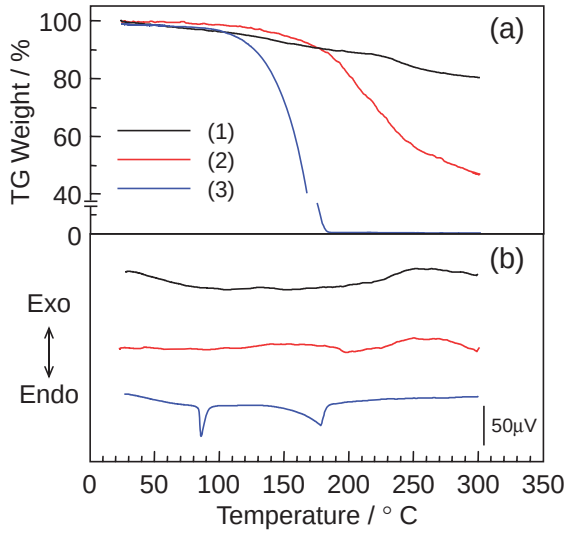

Fig. 1. TG (a) and DTA (b) curves of PVPA–Im composite materials with the heating rate of 10 °C min^{-1} under a dry nitrogen flow. (1) PVPA, (2) PVPA–89 mol % Im, and (3) Im materials (*reproduced from Ref. 63).

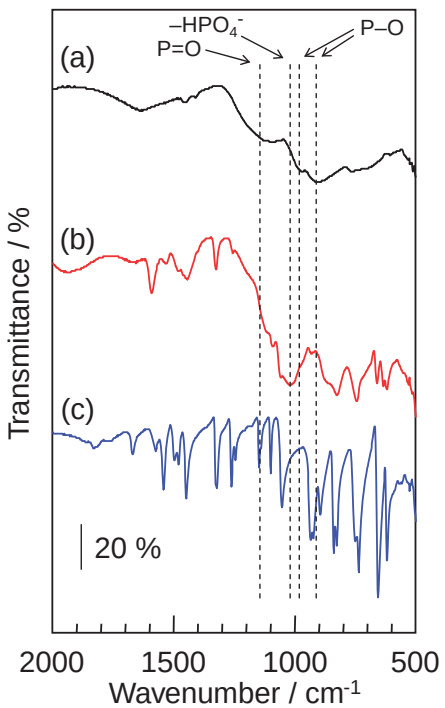

Fig. 2. IR spectra of PVPA–Im composite materials with different mixing ratio of Im. (a) PVPA, (b) PVPA–89 mol % Im, and (c) Im materials (*reproduced from Ref. 63).

tions between phosphonic acid and imidazole molecules that blocks melting as well as structural deterioration of the solid compounds.

Figure 2 shows the IR spectra of (a) PVPA material, (b) PVPA–89 mol % Im, and (c) pure Im materials. The absorption band at 1140 cm^{-1}, which can be attributed to the phosphonyl group (P=O) of PVPA,[54,64–68] disappeared in the PVPA–89 mol % Im composite material. Moreover, the absorption bands at 904 and 983 cm^{-1}, a symmetric and an asymmetric vibration of P–O of PVPA,[54,64–68] decreased as well, although new $–PO_3^{2-}$ band[54,64–68] at 1010 cm^{-1} emerged. The shift of the IR spectra indicated the deprotonation of P–OH group of PVPA, resulting in the formation of anionic P–O$^-$ groups. The stretching band of N–H group,[54,64–69] at ca. 3100 cm^{-1} became larger than that of the pure Im materials[63] as the amount of Im increased (not shown here). These results suggest that P–OH group in acidic polymer deprotonates by the extraction of protons by basic molecules and form anionic P–O$^-$ group. The free proton from P–OH group interacts with non-protonated –N= group of Im molecules and forms a protonated-heterocyclic molecule. It is speculated that proton-transfer reactions between PVPA (acidic polymer) and Im (basic molecule) makes the acid–base ionically paired complex materials, including imidazolium organic salts.

Proton-conducting properties of acid–base composite material were characterized by using a.c. impedance under non-humidified conditions (dry nitrogen flow). The composite materials were sandwiched between two platinum electrodes. Cole–Cole plots of the acid–base composite materials showed a response similar to that of highly ionic-conducting materials.[18–20,70,71] Because these composite materials are electronically insulating, the measured resistance indicates the ionic contributions. There were no other diffusible ions besides protons in the composite material; therefore, we believe that the impedance responses provide true anhydrous proton conduction of the composite materials.

The anhydrous proton conductivities of PVPA–Im composite materials with different Im mixing amount of (□) 61 mol % Im, (■) 76 mol % Im, (○) 83 mol % Im, (●) 89 mol % Im, (◇) 91 mol % Im in temperature range from 80 to 150 °C are shown in Fig. 3. The insert shows the Arrhenius plot of the proton conductivity of PVPA–89 mol % Im composite material. The conductivity of the PVPA–Im composite material increased with the temperature and reached a maximum

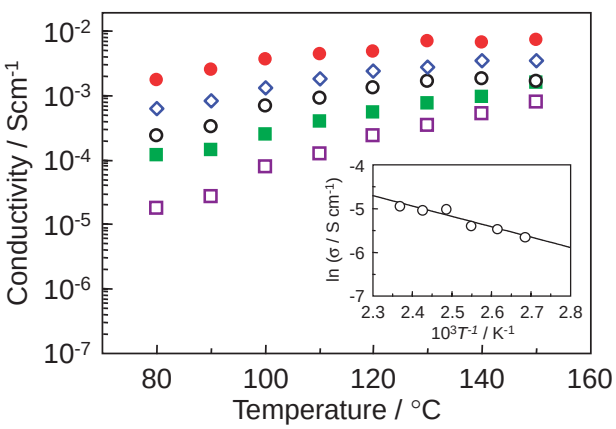

Fig. 3. Proton conductivities of PVPA–Im composite materials with different Im mixing ratios under anhydrous conditions. Conductivities reached a steady-state after the temperature swing of three times. Mixing ratios of Im are □, 61 mol %; ■, 76 mol %; ○, 83 mol %; ●, 89 mol %; and ◇, 91 mol %, respectively. The insert shows Arrhenius plots for PVPA–89 mol % Im composite material (*reproduced from Ref. 63).

conductivity of 7×10^{-3} S cm^{-1} at 150 °C, although the proton conductivities were sensitive to the molar ratio of the heterocyclic molecules. Similar Arrhenius plots for various composition ratios were linear over all temperatures. The activation energies (E_a) of the series of these composites were similar, which suggests that the proton-conducting mechanism must be same unless the imidazole molecules are involved. The Arrhenius formula for anhydrous proton conductivity is described as follows:

$$\sigma = A \exp\left(\frac{-E_a}{k_B T}\right), \quad (1)$$

$$\ln \sigma = \ln A + \left(\frac{-E_a}{k_B T}\right), \quad (2)$$

where σ = anhydrous proton conductivity, A = frequency factor, k_B = Boltzmann constant, and T = absolute temperature. Using to this equation, the value of E_a for proton transfer in the acid–base composite materials was estimated to be 0.22–0.34 eV. These values are almost one order of magnitude higher than the proton conduction in the Nafion® membrane,[70,71] and almost the same as other anhydrous proton conductors, such as solid oxides electrolytes[33,72–74] and fullerene derivatives.[75,76] The value of this activation energy suggests that proton transport in the acid–base composite materials is not assisted by the liquid-like motion of vehicular molecules, but occurs directly in the solid-state matrix.

Proton-transfer and proton-conducting mechanisms of heterocycles under water-free conditions have been reported.[77–80] In these cases, a Grotthuss-type diffusion mechanism has been proposed, in which proton transfer occurs from protonated molecules to neighboring non-protonated molecules. Namely, protonated and non-protonated nitrogen atoms in the heterocycles may act as donors and acceptors in proton-transfer reactions. So, we performed conductivity measurements on various heterocycles with the different acid dissociation constant (pK_a) values. Table 1 shows the pK_a values of various heterocycle molecules.[81] Figure 4 shows the proton conductivity of composite materials with various heterocycle molecules of different pK_a values at 150 °C under anhydrous conditions. Clearly, the conductivity of PVPA–Im composite material is larger than the others, such as PVPA–Py and PVPA–MeIm composite materials. These results suggest that proton conductivity is related to the pK_{a1} value and the number of protonation site in heterocycle molecules. In fact, the Im molecule with two protonation sites has been reported to assemble into a molecular cluster, consisting of ca. twenty molecules[81] through intermolecular hydrogen-bonding. Therefore, PVPA–Im composite material might possess fast proton transfer. However, MeIm molecule, which has only one protonation site, does not form a molecular assembly, which would lead to fast proton transfer, due to a weak intermolecular interactions. These results suggest that the basicity and assembled structure of heterocycle in acid–base composite material are crucial for the formation of the proton-conducting pathways if there are no liquid vehicular molecules present and at intermediate temperature conditions.

Table 1. Dissociation Constants (pK_a Values) of Various Heterocycle Molecules

Heterocycles	pK_a value of heterocycle	
	pK_{a1}	pK_{a2}
Im	7.2	14.5
Py	2.5	14
MeIm	7.4	

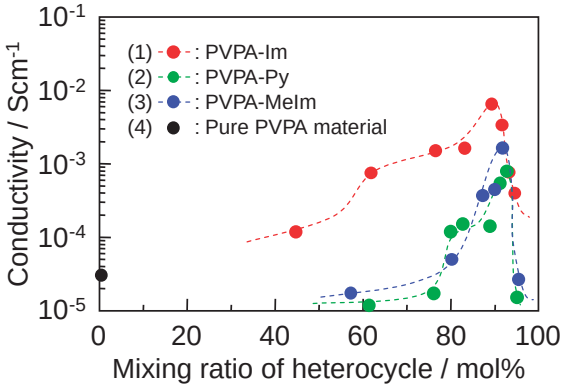

Fig. 4. Proton conductivities of PVPA–heterocycle composite materials at 150 °C with various heterocycle molecules. (1) PVPA–Im, (2) PVPA–Py, (3) PVPA–MeIm, and (4) pure PVPA materials (*reproduced from Ref. 63).

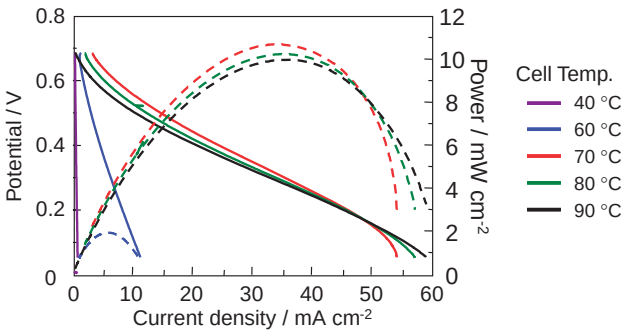

Fig. 5. Current–voltage (I–V) and current–power (I–W) characteristics of the fuel cell employing the PVPA–89 mol % Im composite electrolytes and E–TEK® Pt/C electrode (Pt loading 20 wt %) under the cell operation temperature from 40 to 90 °C and anhydrous (dry H_2/O_2) conditions.

Figure 5 shows current–voltage (I–V) and current–power (I–W) characteristics of the fuel cell employing the PVPA–89 mol % Im composite electrolytes and E–TEK® Pt/C electrode (Pt loading 20 wt %) under the cell operation temperature from 40 to 90 °C and anhydrous (dry H_2/O_2) conditions. The open circuit voltage (OCV) was ca. 0.75 V. Additionally, the maximum power density was approximately 10 mW cm^{-2} at a current density of 35 mA cm^{-2}. The anhydrous conductivity of the MEA with composite material can be estimated from the I–V characteristics. Therefore, the calculated anhydrous conductivity was 5×10^{-4}–1×10^{-3} S cm^{-1} at 80 °C, for example. These conductivities at 80 °C are almost same as the anhydrous conductivity data from the impedance method (see Fig. 3). Therefore, the conductivities in Fig. 3 indicate the same substantial anhydrous proton conductivities across the electrolyte membrane as in the fuel cell operations.

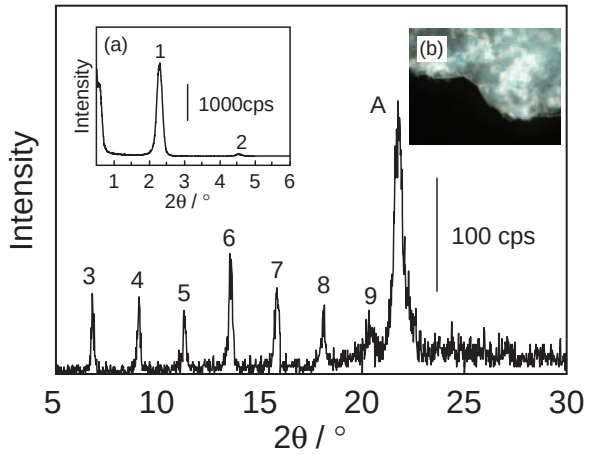

Fig. 6. XRD patterns of UI–MDP composite materials with inserts of (a); the XRD patterns at low-angle regions and (b); the polarized light microscopic image, respectively (*reproduced from Ref. 82).

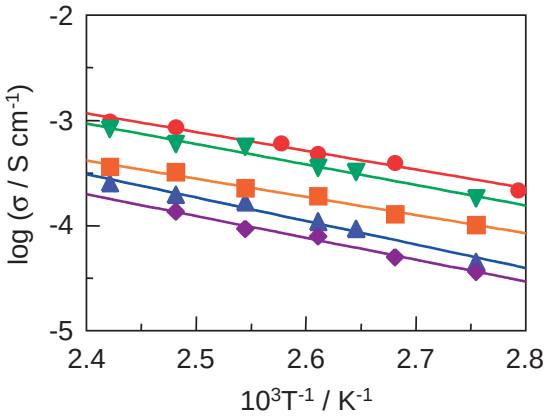

Fig. 7. Arrhenius plots of the proton conduction of UI–MDP composite materials under anhydrous condition. Mixing ratios of MDP are ▲, 10 wt %; ●, 12.5 wt %; ▼, 15 wt %; ■, 20 wt %; and ◆, 50 wt %, respectively (*reproduced from Ref. 82).

2. Self-Assembled Proton Conductor

2.1 Proton-Conducting Pathway with Self-Assembled Structure. Proton transport without the assistance of diffusible molecules,[33–35] such as oxonium ions, phosphoric acid, or sulfuric acid, is important for an anhydrous proton conductor. Additionally, the mixing of acidic and basic molecules is also effective (please, see Section **1**). Furthermore, the proton-conducting pathway in the conductive material is important. So, we prepared a self-assembled acid–base complex consisting of an acidic surfactant, mono-dodecylphosphate (MDP), and a basic surfactant, 2-undecylimidazole (UI), with long hydrophobic chain.[82] The UI–MDP composite material possessed self-assembled lamellar structures, which may act as an effective proton conductive pathway.

The molecular structures of MDP and UI are shown in Scheme 1. The UI–MDP composite material was prepared by mixing UI and MDP solutions. Figure 6 shows the X-ray diffraction (XRD) pattern of UI–MDP composite material in high angle region. Inserts (a) and (b) in Fig. 6 are the XRD patterns in the low-angle region and a polarized light microscopic image of UI–MDP composite material, respectively. Fundamental and associated higher order diffraction peaks suggest that highly ordered lamellar structures formed in UI–MDP composite material. The *d*-spacing of 39.9 Å, which was calculated using Bragg's equation, is almost equivalent to summation of the length of UI and MDP molecules. In contrast, the distance between the alkyl chains was calculated to be 4.09 Å (peak A in Fig. 6). In addition, the lamellar structure was found throughout the composite (see polarized light image).

The proton conductivities of UI–MDP composite materials, measured by using the impedance methods, with MDP mixing ratios of (▲) 10 wt %, (●) 12.5 wt %, (▼) 15 wt %, (■) 20 wt %, and (◆) 50 wt %, respectively, are shown in Fig. 7. The proton conductivity of the composites depended on the mixing ratio of MDP molecules. Especially, UI–12.5 wt % MDP composite material (mole ratio; UI:MDP = 9.6:1) showed the highest conductivity of 1×10^{-3} S cm^{-1} at 150 °C under anhydrous conditions among the series. In contrast, the composite material of imidazole molecule and MDP, which did not form a well-ordered lamellar structure, exhibited a low proton conductivity under anhydrous conditions.

The activation energies (E_a) for the conduction in the lamellar structures estimated from the slop of Arrhenius plot were in the range of 0.30–0.45 eV. This value is almost the same as for other materials reported as anhydrous single proton conductors.[33,62,63,72–76,83] These results indicated that the proton-transporting mechanism in UI–MDP composite material with lamellar structure is, perhaps, not a vehicular mechanism with a diffusible carrier molecules, such as H_3O^+ or $H_5O_2^+$, but a proton hopping Grotthuss-type mechanism. Figure 8 shows a plausible mechanistic model for the two-dimensional proton conduction within the layered molecular space of the surfactant head groups of the UI–MDP lamellar composite material. The UI and MDP molecules assembled to form a lamellar structure with a *d*-spacing of ca. 40 Å. In addition, the distance between alkyl chains of UI and MDP molecules was ca. 4 Å. Addition, the self-assemble surfactant's head group, such as imideoale or phosphonic acid groups, provides fast proton-conducting pathway through direct hopping between the neighboring donor and acceptor sites. The proton-conducting mechanism in the self-assembled structure is thought to be as follows: The imidazole groups are protonated by proton transfer from neighboring phosphate groups and form an acid–base complex. These ionic acid–base complexes can form in various mixing ratios of acidic molecules and heterocyclic molecules. Proton transport in the self-assembled structure occurs from a protonated imidazole group (proton donor) to a non-protonated neighboring imidazole group (proton acceptor). Because fast translocation of the protons needs a smaller energy barrier of activation, the close packing structure and the highly ordered assembly of the acid–base head groups in the lamellar structure might reduce the activation energy and play an important role to afford rapid proton transfer. As a result, the UI–MDP composite material had a high proton conductivity of 1×10^{-3} S cm^{-1} at 150 °C under anhydrous conditions. Therefore, the control of proton-conducting path-

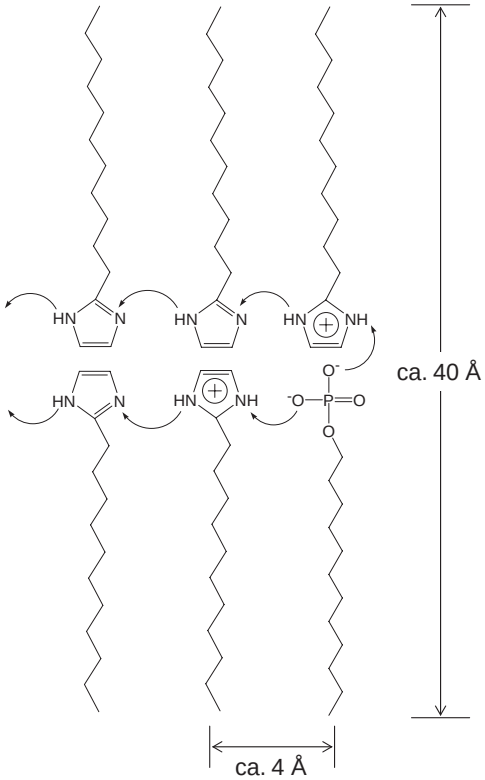

Fig. 8. Mechanistic model for two-dimensional proton conduction within the layered molecular spaces of surfactant head groups of UI–MDP lamellar composite material.

way in acid–base composite materials is an important factor in obtaining anhydrous proton conduction.

2.2 Proton-Conducting Organic Crystal. Solid-state proton-conducting crystals with conductivities of a practical level are very interesting in molecular science for application as electrolytes in PEFCs. Although many investigations have been reported on inorganic crystals, few have been on entirely organic crystals to date. Therefore, control of the proton conduction in an organic crystal with arranged multi-dimensional ionic-conducting paths is not only interesting from the viewpoint of the fundamental materials science of solid-state ionics but also from the viewpoint of the energy technology. So, we have investigated zwitterionic-type proton-conducting organic crystals as the anhydrous electrolyte, because the molecules have acidic and basic sites in their unit structure, meaning that a binary mixture is not necessary.[84] In particular, we studied the protonic properties of 3-pyridinesulfonic acid (PS) as an example of the zwitterionic-type molecular solid. Pure PS exhibited a proton conductivity on the order of 10^{-5} S cm^{-1} at 160 °C under anhydrous condition. This conductivity was not high for the anhydrous proton conductor. However, surprisingly, the anhydrous proton conductivity increased up to about 10^{-3} S cm^{-1} by adding a secondary complex, methylenediphosphonic acid (MP).

The chemical structures of PS and MP are shown in Scheme 1. PS–MP composite materials were prepared by mixing in an agate mortar. These powder samples were compacted into pellets using a hand press. The proton conductive measurements of the PS–MP composite materials were performed

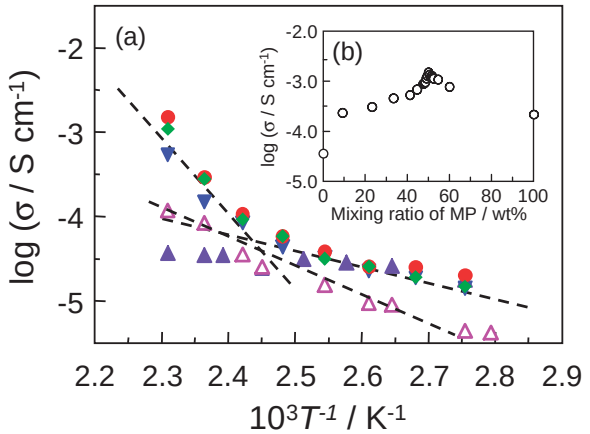

Fig. 9. Arrhenius plots of proton conductivities of PS–MP composite materials with different MP mixing ratios under anhydrous conditions. Mixing ratios of MP were ▲, 0 wt %; ▼, 41 wt %; ●, 50 wt %; ●, 54 wt %; and △, MP materials (*reproduced from Ref. 84).

under a dry nitrogen flow. Typical Cole–Cole plots of PS–MP composite materials showed a feature similar to that of highly ionic conducting membranes. In contrast, according to the TG-DTA, diffusible ions other than protons do not exist in the composite materials (data not shown). Therefore, the impedance response represents the anhydrous proton conductivity. Arrhenius plots of PS and PS–MP composite materials are shown in Fig. 9a, where the plot of (▲), (▼), (●), (◆), and (△) indicate the conductivities of pure PS, PS–41 wt % MP, PS–50 wt % MP, PS–54 wt % MP, and pure MP materials, respectively. The anhydrous proton conductivity of the pure PS material increased with the temperature and reached a maximum conductivity of 4×10^{-5} S cm^{-1} at 160 °C; however, it is not high enough for use as an electrolyte in a fuel cell. So, we mixed PS with MP, which has a large proton-exchange capacity, thus increasing the proton-carrier density. As a result, surprisingly, the anhydrous proton conductivity abruptly increased. Figure 9b shows the anhydrous proton conductivity at 160 °C of the composite material as a function of MP mixing ratios. The conductivity increased with the MP mixing ratio and reached a maximum conductivity of ca. 2×10^{-3} S cm^{-1} at a mixing ratio of 50 wt % MP. Additionally, we have tested the long-term thermal stability of the materials and found a conductivity greater than 10^{-3} S cm^{-1} was maintained at 160 °C for 2 days. Therefore, binary zwitterionic-type molecular solids can be recognized as a thermostable proton-conducting materials, which can be distinguished from other very anhydrous proton conductors, like metal oxides[33,72–74] or inorganic materials,[85–88] such as perovskite-type oxides or super protonic conductor, $CsHSO_4$, reported so far.[84]

The E_a for proton transfer in the PS–MP composite materials was estimated from the slope of Arrhenius plots. The plots for pure PS and MP were almost linear in the experimental temperature ranges, which suggest that one dominant proton-conducting mechanism prevails in the individual pure material with a constant activation energy (E_a). This is comprehensible in the light of simple molecular structures and an absence of a phase transition. Because the molecular structure is quite different, pure PS and MP materials have different value of

E_a (0.10 and 0.65 eV at 80–160 °C, respectively). A value of E_a of 0.1 eV is very small for a solid-state proton conductor, over though there is no mobile liquid molecules in the molecular crystals. However, surprisingly, the PS–MP composite materials had two different activation value of E_a, 0.37–0.45 and 0.86–1.61 eV, in low- and high-temperature regions, respectively. These two E_as indicate that the proton-conducting mechanisms are different in the respective regions. Namely, PS–MP composite material has two parallel proton-conducting pathways. The E_a of ca. 0.4 eV in low-temperature region is one order of magnitude higher than that of Nafion® membrane[70,71] and almost the same as anhydrous proton conductors.[33,62,63,72–76,82] However, the E_a in the high-temperature region is much larger than that of other reported materials and closes to the activation energy of ion conduction in the oxide materials.[35,74]

Proton transfer in heterocycles was based on a hopping mechanism, including Grotthuss-type diffusion of protons, and the E_a was approximately 0.3 eV. In fact, a similar value of E_a for heterocycle molecules in sulfonated poly(ether-ether-ketone) (S-PEEK)–Im or –Py composite materials has been reported.[35] In this research, E_a of ca. 0.3 eV was almost the same as that of PS–MP composite material in low-temperature region. Therefore, the proton-conducting mechanism in the low-temperature region is mainly dominated by the motion of the PS molecules with heterocyclic ring. Figure 10a shows one plausible proton-conducting scheme for the PS molecular crystals, in which proton hopping from sulfonic acid group to pyridine ring occurs first and the rotation (Grotthuss-type mechanism) of pyridine ring occurs second. Therefore, the net transport of a proton can occur from protonated heterocyclic molecules to non-protonated neighbor heterocyclic molecules. The protonated and non-protonated nitrogen in the heterocycles may act as donors and acceptors in proton-transfer reactions. On the other hand, the E_a in the high-temperature region is very large, 0.86–1.61 eV, and the conducting pathway is different from that of heterocyclic PS molecules. However, a phase transition or construction of PS–MP composite phases in the high-temperature region could not be detected by using IR and XRD measurements after heating at 150 °C for 6 h or 170 °C for 6 h. Therefore, proton conduction in the binary materials in the high-temperature region might be ascribed to the MP phases. Figure 10b shows a possible proton conducting scheme in the MP molecules. Although the activation energy is large, proton transfer in the high-temperature region can occur from the neighboring proton to the proton defect sites in MP molecule. Especially, there are four mobile protons in the MP molecules. The acid dissociation constant (pK_a values) of each proton in the MP molecules is different. Therefore, the proton defects and the free protons increase with the temperature, and the proton-transfer reaction between phosphonate groups must be thermally activated, because the energy barrier is larger than that in the PS phase.

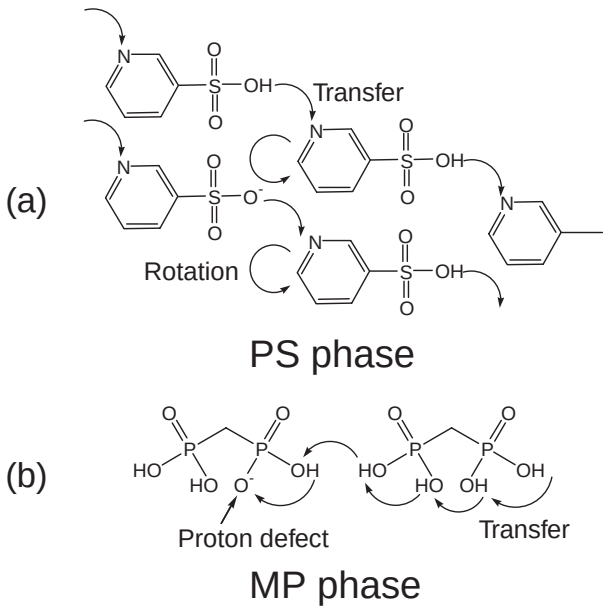

Fig. 10. Proposed proton-conducting mechanism of PS–MP composite material where (a) and (b) showed the individual conduction in the PS and MP phase, respectively. Arrows indicated the direction of proton transfer or molecular rotation.

3. Biomolecular Composite Proton Conductor

3.1 Proton Conductor Employing Chitin. Generally, humidified Nafion® membranes are unstable at higher temperatures (>100 °C) and proton conductivity abruptly decreases. This is due to the evaporation of water molecules from the membrane and the destruction of the molecular structure by irreversible reactions.[4–14] Additionally, the production cost of perfluorinated sulfonic acid membranes is extremely high. Therefore, these factors make it difficult for their industrial application in PEFCs. Therefore, an anhydrous proton-conducting membrane with a low production cost, high proton conductivity, and high stability at intermediate temperatures (100–200 °C) can offer multiple technological advantages for advanced membranes.[89,90]

Chitin, a mucopolysaccharide composed of *N*-acetyl-D-glucosamine, is known to be present abundantly in nature as an essential supporting structure for several living organisms, including fungi, algae, annelids, mollusks, and arthropods. Additionally, chitin-enriched materials, such as crab and shrimp shells, are often discarded as waste. Furthermore, chitin is a biodegradable, non-toxic, and low-cost polymer. Therefore, chitin has been used for bio- or medical-materials, such as a biodegradable materials, sutures in surgical operations, tissue engineering materials, surgical tapes, and artificial skin.[38–42] However, applications of biopolymers, such as chitin, as an engineering material, have been scarcely reported as far as we know. Applications of chitin in electrical devices are not only interesting for material science but also important for environmental science, energy science, and resource science. Additionally, the production cost is lower by using a biopolymer, which was discarded as waste, instead of expensive engineering-polymers. Therefore, the utilization of chitin, which is a well-known biopolymer, as an electrolyte membrane is highly advantageous. So, we prepared an anhydrous proton conductor employing the chitin phosphate (CP), a chitin derivatives, and imidazole (Im), a heterocyclic compound.[91] Here, CP and Im molecules are an acidic polymer and a basic molecule, respectively.

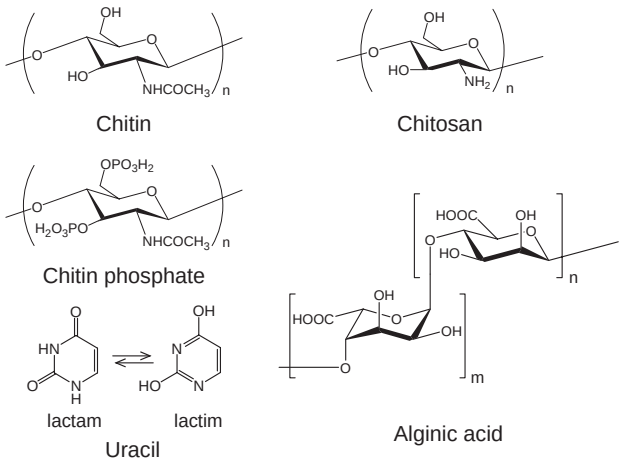

Scheme 2. Molecular structures of various biomolecules.

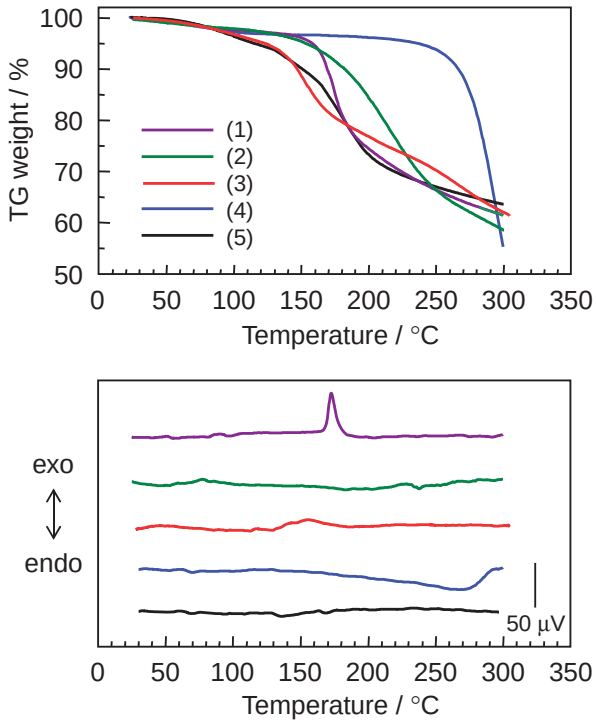

Fig. 11. TG (a) and DTA (b) curves of biopolymer composite materials for (1) pure CP material, (2) CP–200 wt % Im composite material, (3) CP–50 mol % U composite material, (4) CT–200 wt % MP composite material, and (5) AA–Im ($R = 2$) composite materials, respectively (*reproduced from Refs. 91, 94, 95, and 98).

The molecular structures of these biopolymers are shown in Scheme 2. Chitin phosphate (CP) was synthesized by using a previously reported method.[92,93] The degree of phosphorylation (DS) of chitin was determined by using elemental analyses (C, H, and N elements) and inductively coupled plasma (ICP) atomic emission spectrophotometry (P element). In this research, we used 100% phosphorylated chitin. Figure 11 shows (a) TG and (b) DTA curves of various biopolymer composite materials with (1) pure CP material, (2) CP–200 wt % Im composite material, (3) CP–50 mol % U composite material, (4) CT–200 wt % MP composite material, and (5) AA–Im ($R = 2$) composite materials, respectively (*reproduced from Refs. 91, 94, 95, and 98).

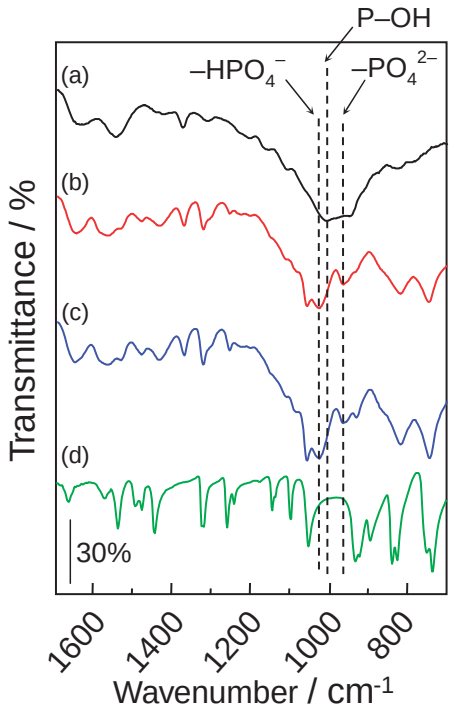

Fig. 12. IR spectra of CP–Im composite materials with different mixing ratio of Im molecules as (a) pure CP, (b) CP–200 wt % Im, (c) CP–500 wt % Im, and (d) pure Im materials, respectively (*reproduced from Ref. 91).

The molecular structures of CP–Im composite materials were characterized by using IR analysis. Figure 12 shows the IR spectra of (a) CP, (b) CP–200 wt % Im, (c) CP–500 wt % Im, and (d) Im materials, respectively. The absorption band at 1011 cm^{-1} was attributed to the asymmetric stretching vibration of P–OH group.[62,63,67,69] This band decreased when basic Im molecules were mixed with the acidic CP material, and two new absorption bands appeared at 1028 and 967 cm^{-1}, the stretching vibration band of $–HPO_4^-$ and $–PO_4^{2-}$,[49,62,63] respectively. This phenomenon has been reported for PVPA–Im composite materials (please see Fig. 2). The data indicats that P–OH group of acidic CP material deprotonates upon mixing with basic Im and forms a $P–O^-$ group. On the other hand, the absorption band at ca. 3100 cm^{-1}, which is the stretching band of N–H group,[62,63,69] also increased (data not shown). These results suggest that free proton from the P–OH group strongly interacts with the non-protonated –N= group of basic Im and form a protonated-heterocyclic molecule. Therefore, the composite material from mixing CP and Im produce

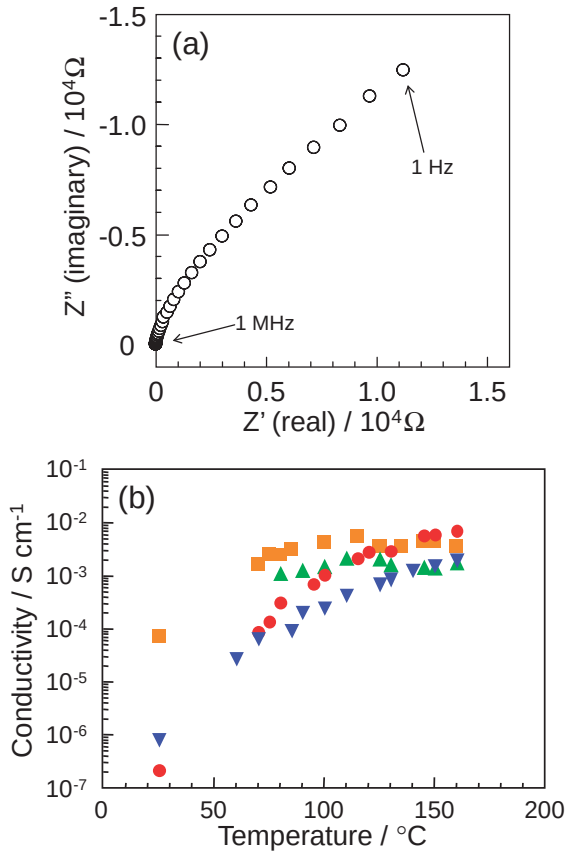

Fig. 13. (a) Typical impedance response (Cole–Cole plots) of CP–200 wt % Im composite material under anhydrous condition. The frequency range is 1 Hz to 1 MHz. (b) Proton conductivities of biopolymer composite materials. (●) CP–200 wt % Im composite material, (▼) CP–50 mol % U composite material, (■) CT–200 wt % MP composite material, (▲) AA–Im ($R = 2$) composite materials (*reproduced from Refs. 91, 94, 95, and 98).

an acid–base salt and, as a result, become more themo-stable than pure CP or Im materials (see TG-DTA in Fig. 11).

Proton conductivity measurements of the CP–Im composite materials were performed by using an a.c. impedance method in the frequency range from 1 Hz to 1 MHz under a dry nitrogen flow. Cole–Cole plots of the CP–Im composite materials, which is quite similar to that of Nafion®,[70,71] inorganic proton conductor, and our anhydrous proton conductors,[82,84] are shown in Fig. 13a. The anhydrous proton conductivities of the biopolymer composite materials in the temperatures range from RT to 160 °C are shown in Fig. 13b. Proton conductivities of (●) CP–200 wt % Im composite material, (▼) CP–50 mol % U composite material, (■) CT–200 wt % MP composite material, and (▲) AA–Im ($R = 2$) composite materials are shown. The anhydrous proton conductivity of the CP–200 wt % Im composite material increased with the temperature and reached a maximum conductivity of 7×10^{-3} S cm^{-1} at 150 °C. The conductivity is highest among the various biopolymers in the present studies. In contrast, the CP membrane did not show any measurable proton conductivity ($<10^{-8}$ S cm^{-1} at 150 °C) (data not shown). These results suggest that biopolymer–heterocycle composite material becomes proton conductive by forming acid–base ionic pairs.

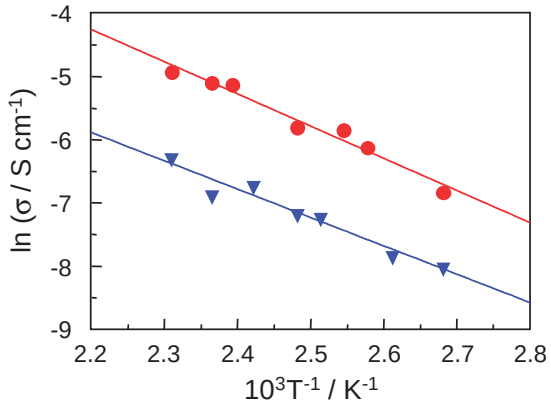

Fig. 14. Arrhenius plots of proton conductivities of biopolymer composite materials. (●) CP–200 wt % Im composite material, (▼) CP–50 mol % U composite material (*reproduced from Refs. 91 and 98).

Next, we determined the E_a of proton transfer in CP–200 wt % Im composite material (Fig. 14 (●)). The change in conductivity was liner in this temperature region. The calculated E_a from the Arrhenius plots of the conductivities was approximately 0.4–0.6 eV. This value is almost the same as other materials reported as anhydrous single proton conductors.[63,82] These results suggest that proton transfer in CP–Im composite material is based on an anhydrous proton-conducting mechanism without the assistant of diffusible carrier, such as oxonium ions. Proton transfer in CP–Im composite material can occur from protonated Im molecules to non-protonated Im molecules. This phenomenon has been reported for various acidic molecule–heterocycle composite materials, such as PVPA–Im or PS–MP composite material. Namely, since the P–OH group in CP can produce an active free proton, the acidic group plays a role in the proton donor[33–35,63,82,83] to Im molecules, and proton transfer in the composite material occurs between the Im molecules. As a result, the CP–Im composite material have a high anhydrous proton conductivity of 7×10^{-3} S cm^{-1} at 150 °C. The biopolymer composites of CP–U have shown the similar proton conducting properties as shown in Fig. 14 (▼).

3.2 Various Biopolymers as Proton Conductor. We also prepared other biomolecule composite proton conductors, such as chitosan (CT)–MP[94] and alginic acid (AA)–Im[95] composite materials. Chitosan (β-1,4-poly-D-glucosamine) is a deacetylated chitin, and alginic acid (linear chains of 1,4′-linked β-D-mannuronic acid and α-L-guluronic acid) is an organized elements of marine algae. The molecular structures are shown in Scheme 2. From the TG-DTA data, these biopolymers were stable at intermediate temperatures (≤150 °C) (see (4) and (5) in Fig. 11). However, the biopolymers themselves did not show any measurable proton conductivity ($<10^{-8}$ S cm^{-1} at 160 °C). So, we prepared the acid–base composite material employing a basic chitosan or an acidic alginic acid. Figure 13b (■) and (▲) shows the anhydrous proton conductivity of CT–200 wt % MP composite materials and AA–Im ($R = 2$) composite material, respectively. The CT–MP composite material showed a high proton conductivity ($>10^{-3}$

$S\,cm^{-1}$) from 70 to 150 °C under anhydrous conditions. This composite has a larger conductivity than the others below 100 °C. Additionally, the proton-conducting mechanism of the CT–MP composite material was due to proton transfer from the phosphonic acid group in MP to a proton defect site, such as P–O^-, without the assistance of diffusible carriers, such as oxonium ions. On the other hand, AA–Im composite material showed a proton conductivity of $2 \times 10^{-3}\,S\,cm^{-1}$ at 130 °C under anhydrous conditions. The E_a of proton transfer in AA–Im composite was 0.2–0.4 eV, and it is almost the same as these of anhydrous proton conductor with the heterocyclic molecules.[62,63,82,84,91] Therefore, the proton-conducting mechanism of the AA–Im composite material is due to the anhydrous proton transfer between heterocycle molecules. These results suggest that the composite material of the biological product, such as biopolymer, and the artificial molecule has a potential for the anhydrous proton conductor as the electrolyte in PEFC.

3.3 Biomembranes as Proton Conductor. Uracil is one of the most important genetic materials in ribonucleic acid (RNA).[96] Although nucleic acids, such as uracil, have been investigated in molecular biology, genetic engineering and biochemistry,[97] uracil has many interesting characteristic properties, such as tautomerism and thermal stability. Additionally, nucleic acid-enriched materials are often discarded as industrial waste. So, we prepared a proton conductive biomembrane consisting of uracil (U) and chitin phosphate (CP).[98] Since this biomembrane did not contain an artificial substrate, it is environmentally safe. Therefore, the biomembrane exhibiting proton conduction may have a potential for the electrolyte of disposable fuel cells.

The molecular structure of uracil is shown in Scheme 2. Uracil have been known to arrange a lactam structure under neutral conditions and a lactam–lactim structure (lactam–lactim tautomerism) under acidic conditions.[99,100] From TG-DTA data, the CP–50 mol % U composite material was stable at the intermediate temperatures (≤150 °C) (see (3) in Fig. 11). The IR spectra of (a) pure CP material, (b) CP–50 mol % U, (c) CP–100 mol % U, and (d) pure U materials are shown in Fig. 15. Spectra (b) and (c) are differential spectrum. The absorption band of the CP–U composite materials at 1550–1700 cm^{-1}, attributed to the lactam form,[69,91,97] was small in comparison to that of pure U. Additionally, the absorption band at 1100 cm^{-1}, attributed to the lactim form, was observed in the CP–U composite materials. In contrast, two new absorption bands at 1070 and 920 cm^{-1}, the stretching vibration of $-HPO_4^-$ and $-PO_4^{2-}$,[62,63,67,69,91,97] respectively, appeared after mixing with U. This indicates the deprotonation of the phosphate groups in CP by U. Similar effects have been obtained for PVPA–Im and CP–Im composite materials. These results suggest that the molecular structure of U in the CP–U composite materials partially changes from the lactam form to lactim form (i.e., lactam–lactim tautomerism) by addition of a free proton from the acidic CP. Lactam–lactim tautomerism in acid–base composite material has also been reported to occur in a U–mono-dodecylphosphate (MDP) composite material.[97]

The anhydrous proton conductivities of the CP–50 mol % U composite materials are shown in Fig. 13b (▼). The anhydrous proton conductivity of the CP–50 mol % U composite material increased with the temperature and reached a maximum conductivity of $2 \times 10^{-3}\,S\,cm^{-1}$ at 160 °C. Figure 14 (▼) shows the Arrhenius plots of the proton conductivity for the 50 mol % U composite material. The E_a of the conduction estimated from the slop were 0.5–0.7 eV and are about one order of magnitude higher than that of the Nafion® membrane.[70,71] This E_a value is two to three times higher than that of heterocyclic molecules. These results imply that this proton transfer in CP–U composite material has a higher energy barrier for Grotthuss-type diffusion than that in other molecules. This is, probably, due to the strong-hydrogen-bonding network of U molecules, which have many hydrogen-bonding sites. Transport of the proton in the hydrogen-bonded U networks can possibly occur from protonated U molecules (proton donor) to neighboring non-protonated U molecules (proton acceptor). The E_a of this translocation is much higher than the same process in the water, because the rotational motion of U molecules in the hydrogen-bonding network might cause a higher barrier height due to stronger interactions among the U molecules and/or with the CP backbone.

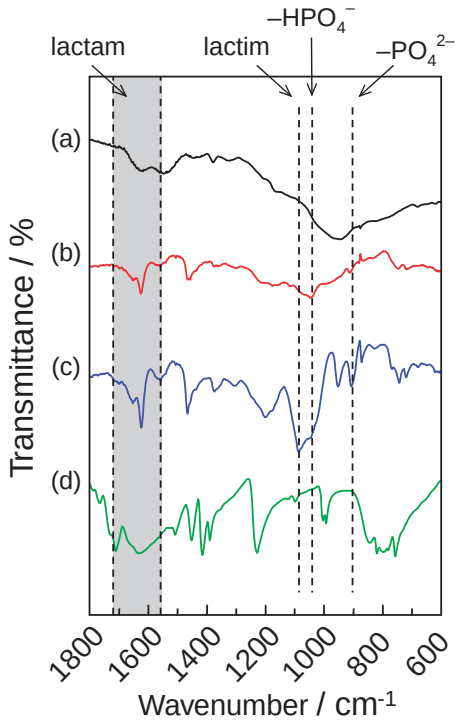

Fig. 15. IR spectra of CP–U composite materials with different mixing ratios of U; (a) pure CP, (b) CP–50 mol % U, (c) CP–100 mol % U, and (d) pure U materials, respectively. The spectrum (b) and (c) are the differential spectra (*reproduced from Ref. 98).

Next, we tested the performance of a fuel cell under H_2/O_2 conditions employing a CP–50 mol % U composite membrane electrode assembly (MEA) as the electrolyte. Figure 16 shows *I–V* and *I–W* characteristics of the MEA at 160 °C under non-humidified conditions (0% RH) and low humidified conditions (10% RH, 20% RH, and 30% RH). An OCV of ca. 0.75 V is lower than the conventional potential for H_2/O_2 cell. Therefore, this indicates that the membrane has a low gas permeabil-

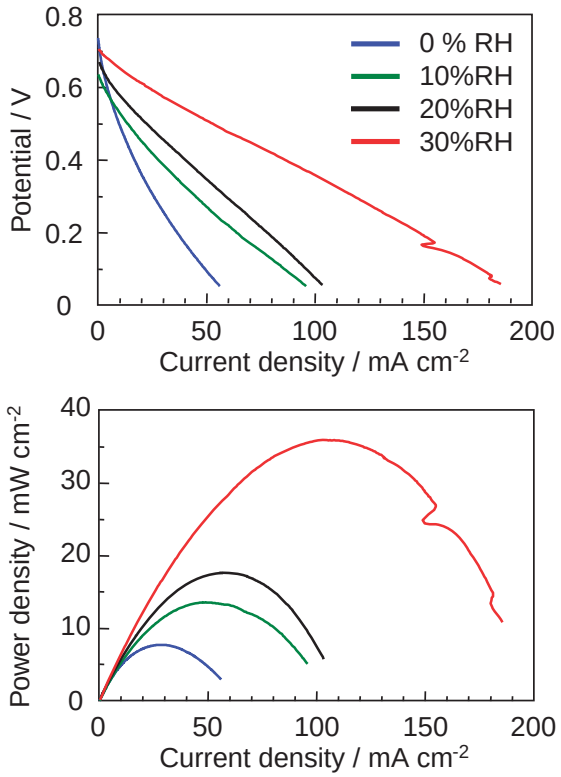

Fig. 16. *I–V* and *I–W* characteristics of the fuel cell employing the CP–50 mol % U composite electrolytes and E–TEK® Pt/C electrode (Pt loading 20 wt %) at 160 °C under non-humidified H_2/O_2 conditions (0% RH) and humidified conditions (10% RH, 20% RH, and 30% RH), respectively.

ity and/or that oxygen reduction by U has a large cathode overpotential. The current densities increased with an increase in the cell temperature (data not shown). The maximum power output was ca. 8 mW cm^{-2} at 160 °C under 0% RH conditions. Additionally, the power output at 160 °C was stable for 24 h under non-humidified H_2/O_2 conditions (data not shown). Finally, we tested the fuel cell performance under low-humidity conditions. The power density of the cell was found to increase with an increase in the humidity, and the CP–50 mol % U composite material had a maximum output of ca. 35 mW cm^{-2} at 160 °C under 30% RH conditions (see Fig. 16). In contrast, the power output of CP–U composite material under H_2/O_2 conditions increased linearly with the relative humidity (data not shown). The increase in the power output with the humidity can be ascribed to the increase of the electrolyte's conductivity. These results suggested that the CP–U composite biomembrane can be used as an anhydrous proton-conducting electrolyte for fuel cells under H_2/O_2 conditions even though they consist of only biological molecules, such as nucleic acids and discarded biopolymers.

4. Conclusion

Several of acid–base composite biopolymer materials were investigated as anhydrous proton-conducting membranes in the present work. The acid–base pairs were shown proved to form proton-conducting pathways by direct proton-transfer reactions between the two moieties, and the membrane exhibited a large conductivity in spite of the absence of mobile liquid molecules, such as water.[77–80] The temperature dependence of the conductivities and activation energy of conduction suggests a novel proton-transfer reaction among the electrochemical network of the acid–base pairs in the solid polymeric materials, which is much different from those in the hydrated protons in water phase. Table 2 summarizes the results of conducting properties of the composite membrane studied in the present work.[62,63,82,84,91,94,95,97,99,101] In most cases, the conductivity ranged from 1×10^{-4} to 1×10^{-2} S cm^{-1}, and the activation energy ranged from 0.2 to 0.5 eV. The maximum conductivity was obtained for polystyrene sulfonic acid/12-phosphotungstic acid (PSS–PWA) composites (1×10^{-2} S cm^{-1} at 180 °C) and the activation energy was 0.4–0.5 eV.[101] It is very interesting that a large anhydrous proton conductivity was obtained at 180 °C, which has never been achieved by ion-exchanged membrane at this temperature due to the drying of the membrane.[101] An anhydrous conductivity of 1×10^{-2} S cm^{-1} at 180 °C is the highest value ever reported for a PEFC electrolyte and should encourage the development of new electrolytes. Also, the high power outputs under dry conditions was also achieved by the MEA these anhydrous proton-conducting membrane; the maximum power output of 8 mW cm^{-2} at 160 °C under anhydrous conditions seems to be the highest also the top record among those reported elsewhere. An anhydrous PEFC cell operation was tested for several cases for different acid–base composite membranes and the composite were shown to be anhydrous proton-conducting electrolytes. Also, the possibility of biomaterials for PEFC application was also demonstrated; the well-known biomaterials Chitosan, Chitin phosphate, and Uracil were shown to possess proton conductivities under anhydrous conditions when mixing with a counter acid or base. A fuel cell electrolyte membrane consisting of only biomaterials was prepared for the first time: these membranes are low-cost and environmentally friendly, and thus, it is advantageous to use them in industrial devices.[91,94,95,97,98] Additionally, the self-assembling properties of the acid–base molecules, including Uracil, helped to form fast conducting proton channels.

However, the problems for the practical applications were raised. An anhydrous conductivity of 10^{-2} S cm^{-1} is large compared to the other investigations, but, still too small for practical use. Usually, a conductivity of 10^{-1} S cm^{-1} is required for high power outputs. Only fast proton-conducting ion-exchanged membranes, such as Nafion®, have been used, because the proton mobility in the liquid phase has been known to be the only mechanism for fast proton transfer in low-temperature electrolyte. An activation energy between 0.2–0.5 eV suggests that strongly bound protons in the acid–base pairs' bonding network of the composite membranes, move by jumping to the next neighboring sites through a thermally actuated diffusion. Direct proton transport between the acid–base couples in the solid-state polymer matrix necessitates an energy because of less than an electron volt transport process due to the electrochemical (proton transfer) reactions. If more suitable molecular pairs are found with a smaller activation energy, the anhydrous proton conductivities should increase and reach at the practical levels. Closely matched of

Table 2. Proton-Conducting Properties of Acid–Base Composite Membranes

Acid–base composite		Molecular structure		Anhydrous proton conductivity	Activation energy
PVPA–Im	Poly(vinylphosphonic acid) Imidazole	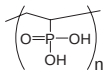		7×10^{-3} S cm^{-1} (at 150 °C)	0.2–0.4 eV
PVPA–Py	Poly(vinylphosphonic acid) Pyrazole	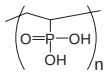		8×10^{-4} S cm^{-1} (at 150 °C)	—
PVPA–MeIm	Poly(vinylphosphonic acid) 1-Methylimidazole	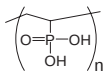	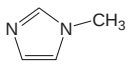	1×10^{-3} S cm^{-1} (at 150 °C)	—
PVPA–UI	Poly(vinylphosphonic acid) 2-Undecylimidazole	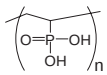	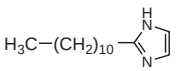	5×10^{-4} S cm^{-1} (at 150 °C)	0.4–1.0 eV
PVPA–PWA	Poly(vinylphosphonic acid) 12-Phosphotungstic acid	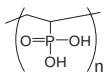	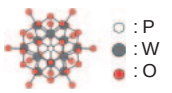	5×10^{-3} S cm^{-1} (at 160 °C)	0.5–0.85 eV
PSS–PWA	Polystyrene sulfonic acid 12-Phosphotungstic acid	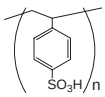	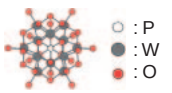	1×10^{-2} S cm^{-1} (at 180 °C)	0.4–0.5 eV
MDP–BnIm	Mono-dodecylphosphate Benzimidazole	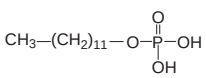		1×10^{-3} S cm^{-1} (at 150 °C)	ca. 0.25 eV
MDP–UI	Mono-dodecylphosphate 2-Undecylimidazole	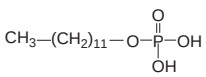	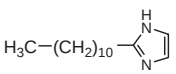	1×10^{-3} S cm^{-1} (at 150 °C)	0.3–0.45 eV
PS–MP	3-Pyridinesulfonic acid Methanediphosphonic acid	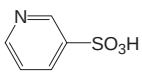	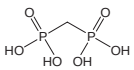	2×10^{-3} S cm^{-1} (at 160 °C)	0.4–1.6 eV
CP–Im	Chitin phosphate Imidazole	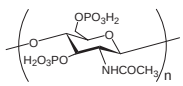		7×10^{-3} S cm^{-1} (at 150 °C)	0.4 eV
CP–U	Chitin phosphate Uracil	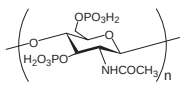	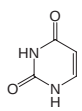	2×10^{-3} S cm^{-1} (at 150 °C)	0.5–0.7 eV
CP–UI	Chitin phosphate 2-Undecylimidazole	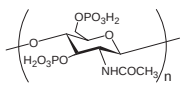	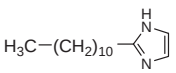	7×10^{-4} S cm^{-1} (at 150 °C)	0.5–1.0 eV
AA–Im	Alginic acid Imidazole	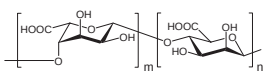		2×10^{-3} S cm^{-1} (at 130 °C)	0.2–0.4 eV
CT–MP	Chitosan Methanediphosphonic acid	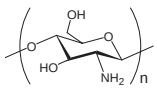	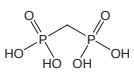	5×10^{-3} S cm^{-1} (at 150 °C)	—
MDP–U	Mono-dodecylphosphate Uracil	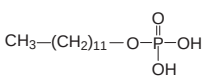	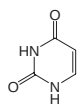	7×10^{-4} S cm^{-1} (at 150 °C)	0.1–0.3 eV
PVS–U	Poly(vinylsulfonic acid) Uracil	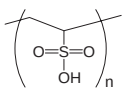	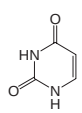	1×10^{-5} S cm^{-1} (at 160 °C)	—

acid and base strengths should result in a much smaller activation energy for having large conductivities. In liquid water, an activation energy of only about 0.02 eV is necessary for prevailing Grotthuss mechanism of proton rotation and transfer, i.e., a hop and turn mechanism of conduction. Additionally, the thermal as well as electrochemical stability should be considered before practical applications, because usually, biomaterials are often fragile and particularly weak to attack by various radicals in electrochemical reactions. Finally, interface charge transfer between the anhydrous membrane and the platinum electrodes is also an important issue for efficient cell operations.

The authors are greatly indebted to New Energy and Industrial Technology Development Organization (NEDO) for financial support and the miscellaneous supports from National Institute of Industrial Science and Technology (AIST).

References

1 L. Carrette, K. A. Friedrich, U. Stimming, *ChemPhysChem* **2000**, *1*, 162.
2 C. Wallmark, P. Alvfors, *J. Power Sources* **2002**, *106*, 83.
3 H. Inaka, S. Sumi, K. Nishizaki, T. Tabata, A. Kataoka, H. Shinkai, *J. Power Sources* **2002**, *106*, 60.
4 J. A. Kerres, *J. Membr. Sci.* **2001**, *185*, 3.
5 M. Rikukawa, K. Sanui, *Prog. Polym. Sci.* **2000**, *25*, 1463.
6 K. D. Kreuer, *J. Membr. Sci.* **2001**, *185*, 29.
7 K. D. Kreuer, *ChemPhysChem* **2002**, *3*, 771.
8 M. F. H. Schuster, W. H. Meyer, M. Schuster, K. D. Kreuer, *Chem. Mater.* **2004**, *16*, 329.
9 G. Alberti, M. Casciola, *Solid State Ionics* **2001**, *145*, 3.
10 Q. Li, R. He, J. O. Jensen, N. J. Bjerrum, *Chem. Mater.* **2003**, *15*, 4896.
11 M. A. Hickner, H. Ghassemi, Y. S. Kim, B. R. Einsla, J. E. McGrath, *Chem. Rev.* **2004**, *104*, 4587.
12 W. H. J. Hogarth, J. C. D. Costa, G. O. Lu, *J. Power Sources* **2005**, *142*, 223.
13 D. J. Jones, J. Rozière, *J. Membr. Sci.* **2001**, *185*, 41.
14 P. Jannasch, *Curr. Opin. Colloid Interface Sci.* **2003**, *8*, 96.
15 C. Yang, P. Costamagna, S. Srinivasan, J. Benziger, A. B. Bocarsly, *J. Power Sources* **2001**, *103*, 1.
16 F. Damay, L. C. Klein, *Solid State Ionics* **2003**, *162–163*, 261.
17 S. P. Nunes, B. Ruffmann, E. Rikowski, S. Vetter, K. Richau, *J. Membr. Sci.* **2002**, *203*, 215.
18 I. Honma, H. Nakajima, O. Nishikawa, T. Sugimoto, S. Nomura, *Solid State Ionics* **2003**, *162–163*, 237.
19 I. Honma, H. Nakajima, O. Nishikawa, T. Sugimoto, S. Nomura, *J. Electrochem. Soc.* **2003**, *150*, A616.
20 H. Nakajima, S. Nomura, T. Sugimoto, O. Nishikawa, I. Honma, *J. Electrochem. Soc.* **2002**, *149*, A953.
21 J. D. Kim, T. Mori, I. Honma, *J. Membr. Sci.* **2006**, *281*, 735.
22 O. Nishikawa, T. Sugimoto, S. Nomura, K. Doyama, K. Miyatake, H. Uchida, M. Watanabe, *Electrochim. Acta* **2004**, *50*, 667.
23 S. M. J. Zaidi, S. D. Mikhailenko, G. P. Robertson, M. D. Guiver, S. Kaliaguine, *J. Membr. Sci.* **2000**, *173*, 17.
24 N. Asano, M. Aoki, S. Suzuki, K. Miyatake, H. Uchida, M. Watanabe, *J. Am. Chem. Soc.* **2006**, *128*, 1762.
25 P. Staiti, M. Minutoli, S. Hocevar, *J. Power Sources* **2000**, *90*, 231.
26 D. Schoolmann, O. Trinquet, J. C. Lassègues, *Electrochim. Acta* **1992**, *37*, 1619.
27 R. W. Kopitzke, C. A. Linkous, H. R. Anderson, G. L. Nelson, *J. Electrochem. Soc.* **2000**, *147*, 1677.
28 J. L. Qiao, N. Yoshimoto, M. Ishikawa, M. Morita, *Electrochim. Acta* **2002**, *47*, 3441.
29 M. Tatsumisago, H. Honjo, Y. Sakai, T. Minami, *Solid State Ionics* **1994**, *74*, 105.
30 P. Staiti, S. Freni, S. Hocevar, *J. Power Sources* **1999**, *79*, 250.
31 M. Yamada, D. Li, I. Honma, H. Zhou, *J. Am. Chem. Soc.* **2005**, *127*, 13092.
32 M. Yamada, M. Wei, I. Honma, H. Zhou, *Electrochem. Commun.* **2006**, *8*, 1549.
33 P. Colomban, A. Novak, *J. Mol. Struct.* **1988**, *177*, 277.
34 K. D. Kreuer, *Chem. Mater.* **1996**, *8*, 610.
35 K. D. Kreuer, A. Fuchs, M. Ise, M. Spaeth, J. Maier, *Electrochim. Acta* **1998**, *43*, 1281.
36 K. Iwata, T. Sawadaishi, S. Nishimura, S. Tokura, N. Nishi, *Int. J. Biol. Macromol.* **1996**, *18*, 149.
37 O. Smidsrød, G. Skjåk-Bræk, *Trends Biotechnol.* **1990**, *8*, 71.
38 M. N. V. R. Kumar, *React. Funct. Polym.* **2000**, *46*, 1.
39 M. Mochizuki, Y. Kadoya, Y. Wakabayashi, K. Kato, I. Okazaki, M. Yamada, T. Sato, N. Sakairi, N. Nishi, M. Nomizu, *FASEB J.* **2003**, *17*, 875.
40 J. K. F. Suh, H. W. T. Matthew, *Biomaterials* **2000**, *21*, 2589.
41 T. Chandy, C. P. Sharma, *Biomater., Artif. Cells, Artif. Organs* **1990**, *18*, 1.
42 I. V. Yannas, J. F. Burke, D. P. Orgill, E. M. Skrabut, *Science* **1982**, *215*, 174.
43 M. Yamada, K. Kato, M. Nomizu, N. Sakairi, K. Ohkawa, H. Yamamoto, N. Nishi, *Chem. Eur. J.* **2002**, *8*, 1407.
44 M. Yamada, K. Kato, K. Shindo, M. Nomizu, M. Haruki, N. Sakairi, K. Ohkawa, H. Yamamoto, N. Nishi, *Biomaterials* **2001**, *22*, 3121.
45 M. Yamada, K. Kato, M. Nomizu, K. Ohkawa, H. Yamamoto, N. Nishi, *Environ. Sci. Technol.* **2002**, *36*, 949.
46 M. Yamada, M. Yokota, M. Kaya, S. Satoh, B. Jonganurakkun, M. Nomizu, N. Nishi, *Polymer* **2005**, *46*, 10102.
47 A. Chernyshev, K. M. Armstrong, S. Cukierman, *Biophys. J.* **2003**, *84*, 238.
48 R. Pomès, B. Roux, *Biophys. J.* **2002**, *82*, 2304.
49 M. Kawahara, J. Morita, M. Rikukawa, K. Sanui, N. Ogata, *Electrochim. Acta* **2000**, *45*, 1395.
50 R. Bouchet, E. Siebert, *Solid State Ionics* **1999**, *118*, 287.
51 X. Glipa, B. Bonnet, B. Mula, D. J. Jones, J. Rozière, *J. Mater. Chem.* **1999**, *9*, 3045.
52 H. G. Herz, K. D. Kreuer, J. Maier, G. Scharfenberger, M. F. H. Schuster, W. H. Meyer, *Electrochim. Acta* **2003**, *48*, 2165.
53 M. F. H. Schuster, W. H. Meyer, G. Wegner, H. G. Herz, M. Ise, M. Schuster, K. D. Kreuer, J. Maier, *Solid State Ionics* **2001**, *145*, 85.
54 A. Bozkurt, W. H. Meyer, *Solid State Ionics* **2001**, *138*, 259.
55 H. Pu, W. H. Meyer, G. Wegner, *Macromol. Chem. Phys.* **2001**, *202*, 1478.
56 M. F. H. Schuster, W. H. Meyer, M. Schuster, K. D. Kreuer, *Chem. Mater.* **2004**, *16*, 329.
57 J. Sun, D. R. MacFarlane, M. Forsyth, *Electrochim. Acta* **2001**, *46*, 1673.
58 J. Sun, L. R. Jordan, M. Forsyth, D. R. MacFarlane, *Electrochim. Acta* **2001**, *46*, 1703.
59 A. Noda, M. A. B. H. Susan, K. Kudo, S. Mitsushima, K. Hayamizu, M. Watanabe, *J. Phys. Chem. B* **2003**, *107*, 4024.
60 M. A. B. H. Susan, A. Noda, S. Mitsushima, M. Watanabe, *Chem. Commun.* **2003**, 938.
61 S. Li, M. Liu, *Electrochim. Acta* **2003**, *48*, 4271.
62 M. Yamada, I. Honma, *Electrochim. Acta* **2003**, *48*, 2411.
63 M. Yamada, I. Honma, *Polymer* **2005**, *46*, 2986.
64 J. Ellis, A. D. Wilson, *Polym. Int.* **1991**, *24*, 221.
65 Y. E. Greish, P. W. Brown, *Biomaterials* **2001**, *22*, 807.

66 Y. E. Greish, P. W. Brown, *J. Am. Ceram. Soc.* **2002**, *85*, 1738.
67 *Topics in Phosphorus Chemistry*, ed. by D. E. C. Corbridge, John Wiely & Sons, New York, **1969**.
68 A. Bozkurt, W. H. Meyer, J. Gutmann, G. Wegner, *Solid State Ionics* **2003**, *164*, 169.
69 *Spectrometric Identification of Organic Compounds*, ed. by R. M. Silverstein, F. X. Webster, John Wiley & Sons, New York, **1998**.
70 T. A. Zawodzinski, C. Derouin, S. Radzinski, R. J. Sherman, V. T. Smith, T. E. Springer, S. Gottesfeld, *J. Electrochem. Soc.* **1993**, *140*, 1041.
71 Y. Sone, P. Ekdunge, D. Simonsson, *J. Electrochem. Soc.* **1996**, *143*, 1254.
72 A. I. Baranov, V. V. Sinitsyn, V. Y. Vinnichenko, D. J. Jones, B. Bonnet, *Solid State Ionics* **1997**, *97*, 153.
73 Y. M. Li, M. Hibino, M. Miyayama, T. Kudo, *Solid State Ionics* **2000**, *134*, 271.
74 H. Iwahara, *Solid State Ionics* **1996**, *86–88*, 9.
75 K. Hinokuma, M. Ata, *Chem. Phys. Lett.* **2001**, *341*, 442.
76 Y. M. Li, K. Hinokuma, *Solid State Ionics* **2002**, *150*, 309.
77 G. R. Goward, M. F. H. Schuster, D. Sebastiani, I. Schnell, H. W. Spiess, *J. Phys. Chem. B* **2002**, *106*, 9322.
78 B. S. Hickman, M. Mascal, J. J. Titman, I. G. Wood, *J. Am. Chem. Soc.* **1999**, *121*, 11486.
79 I. Fischbach, H. W. Spiess, K. Saalwachter, G. R. Goward, *J. Phys. Chem. B* **2004**, *108*, 18500.
80 S. R. Benhabbour, R. P. Chapman, G. Scharfenberger, W. H. Meyer, G. R. Goward, *Chem. Mater.* **2005**, *17*, 1605.
81 *An Introduction to the Chemistry of Heterocyclic Compounds*, 3rd ed., ed. by R. M. Acheson, John Wiley & Sons, Canada, **1976**.
82 M. Yamada, I. Honma, *J. Phys. Chem. B* **2004**, *108*, 5522.
83 Th. Dippel, K. D. Kruer, J. C. Lassègues, D. Rodriguez, *Solid State Ionics* **1993**, *61*, 41.
84 M. Yamada, I. Honma, *Chem. Phys. Lett.* **2005**, *402*, 324.
85 D. A. Boysen, T. Uda, C. R. I. Chisholm, S. M. Haile, *Science* **2004**, *303*, 68.
86 S. M. Haile, D. A. Boysen, C. R. I. Chisholm, R. B. Merle, *Nature* **2001**, *410*, 910.
87 A. I. Baranov, L. A. Shuvalov, N. M. Schagina, *JETP Lett.* **1982**, *36*, 459.
88 A. I. Baranov, V. P. Khiznichenko, L. A. Shuvalov, *Ferroelectrics* **1989**, *100*, 135.
89 N. Ogata, *Kobunshi* **1995**, *44*, 72.
90 M. Wakizoe, O. A. Velev, S. Srinivasan, *Electrochim. Acta* **1995**, *40*, 335.
91 M. Yamada, I. Honma, *Angew. Chem., Int. Ed.* **2004**, *43*, 3688.
92 N. Nishi, S. I. Nishimura, A. Ebina, A. Tsutsumi, S. Tokura, *Int. J. Biol. Macromol.* **1984**, *6*, 53.
93 N. Nishi, A. Ebina, S. I. Nishimura, A. Tsutsumi, O. Hasegawa, S. Tokura, *Int. J. Biol. Macromol.* **1986**, *8*, 311.
94 M. Yamada, I. Honma, *Electrochim. Acta* **2005**, *50*, 2837.
95 M. Yamada, I. Honma, *Polymer* **2004**, *45*, 8349.
96 *Principles of Nucleic Acid Structure*, ed. by W. Saenger, Springer-Verlag, Berlin, **1987**.
97 M. Yamada, I. Honma, *ChemPhysChem* **2004**, *5*, 724.
98 M. Yamada, I. Honma, *Biosens. Bioelectron.* **2006**, *21*, 2064.
99 J. Rejnek, M. Hanus, M. Kabeláč, F. Ryjáček, P. Hobza, *Phys. Chem. Chem. Phys.* **2005**, *7*, 2006.
100 A. R. Katritzky, J. M. Lagowski, *Adv. Heterocycl. Chem.* **1963**, *1*, 2.
101 M. Yamada, I. Honma, *J. Phys. Chem. B* **2006**, *110*, 20486.

Itaru Honma is a Group Leader of Nano-energy materials in the Energy Technology Research Institute, National Institute of Advanced Industrial Science and Technology (AIST). He graduated the Department of Metallurgy and Materials Science, the University of Tokyo in 1984 with a B.S. He became Research Assistant at the Department of Chemical Engineering, the University of Tokyo in 1985 and assistant professor at 1991 in the same department. He move to Electrotechnical laboratory, AIST as a senior researcher at 1995 and became Group Leader, Energy Electronics Institute, AIST in 2001. He has been investigating advanced processing of functional materials and its application to renewable energy devices for global sustainability.

Masanori Yamada was born in Kyoto in 1971. He graduated Doshisha University in 1994 and received Ph.D. degree from Hokkaido University in 1999. From 1999 to 2002, he was a research fellow in Shinshu University. In 2002, he moved to National Institute of Advanced Industrial Science and Technology (AIST), and in 2006, he became an Associate Professor in Okayama University of Science. His research interests include the design of materials, such as proton conductor, energy device, or biomaterial, by using biopolymers and artificial polymers.